Landslide Inventory Map of the Valemount Area, British Columbia, Canada. A Detailed Methodological Description

Txomin Bornaetxea, Andrée Blais-Stevens, and Brendan Miller

Abstract

Landslides are a recurring geomorphological process in high mountainous areas like Valemount in the Canadian Rocky Mountains, British Columbia. The compilation of detailed information about the spatial distribution and characteristics of past landslides is essential for assessing future potential hazards. To provide baseline geoscience information to stakeholders and decision-makers, we carried out a landslide inventory that covers roughly 1200 km^2. Using visual interpretation of aerial orthophotos, a digital elevation model of 5 × 5 m resolution and satellite imagery, we compiled up to 1286 landslides and classified them into 11 categories and three levels of certainty. The current paper describes the mapping methodology and summarizes our results.

Keywords

Landslide inventory • Air photo-interpretation • LiDAR • Valemount • British Columbia

1 Introduction

Natural Resources Canada's Public Safety Geoscience Program (PSG) at the Geological Survey of Canada undertakes research on geohazards such as landslides, earthquakes, tsunamis, volcanoes, and space weather. PSG knowledge products provide baseline geoscience information to stakeholders and decision-makers to reduce the risk to the population and critical infrastructure.

In accordance with the PSG mandate, a landslide inventory was created along the transportation corridor between Moose Lake and Tête Jaune Cache village and continuing north along the Fraser River to Dunster, in east central British Columbia (Fig. 1). The study area covers roughly 1200 km^2 and includes both sides of Robson Valley extending eastward and upstream toward Jasper National Park, Alberta. The study area covers a key transportation corridor in which highways 16 and 5, Canadian National Railway, and an oil pipeline are located. The permanent population density in the study area is low, but the population can increase during summer months by tourists visiting the area.

The elevation within the study area ranges between 720 and 2800 m above sea level. Slope gradient varies from <2° on the alluvial plains at lower elevations to >80° in the high mountainous areas, with the average slope being 22.5°. Upper Proterozoic rocks of the Miette Group underlie the study area (Mountjoy 1980; Massey et al. 2005), with coarse clastic sedimentary rocks including sandstone, conglomerate, argillite, phyllite, diamictite and minor limestone exposed at lower elevations; while mudstone, siltstone and shale are exposed at higher elevations. In the northwest boundary of the study area, the McNaughton Formation is observed, consisting of massive quartz sandstone, siltstone, and minor pebble conglomerate.

The surficial materials on the valley's floor are composed mainly of a mixture of gravelly silts to clayey sands with various quantities of cobbles and boulders, while in the upper zones, colluvium (including debris, talus and scree) and morainal deposits predominate (Ministry of Transportation and Highways (MOTI 1999). The study area is located in a region of low to moderate seismic hazard (NRCan 2015).

T. Bornaetxea (✉)
Department of Geology, University of the Basque Country (UPV/EHU), Leioa, Spain
e-mail: txomin.bornaetxea@ehu.eus

A. Blais-Stevens
Natural Resources Canada, Ottawa, ON, Canada
e-mail: andree.blais-stevens@nrcan-rncan.gc.ca

B. Miller
Ministry of Forests, Prince George, BC, Canada
e-mail: Brendan.Miller@gov.bc.ca

I. Alcántara-Ayala et al. (eds.), *Progress in Landslide Research and Technology, Volume 1 Issue 2, 2022*, Progress in Landslide Research and Technology,
https://doi.org/10.1007/978-3-031-18471-0_27

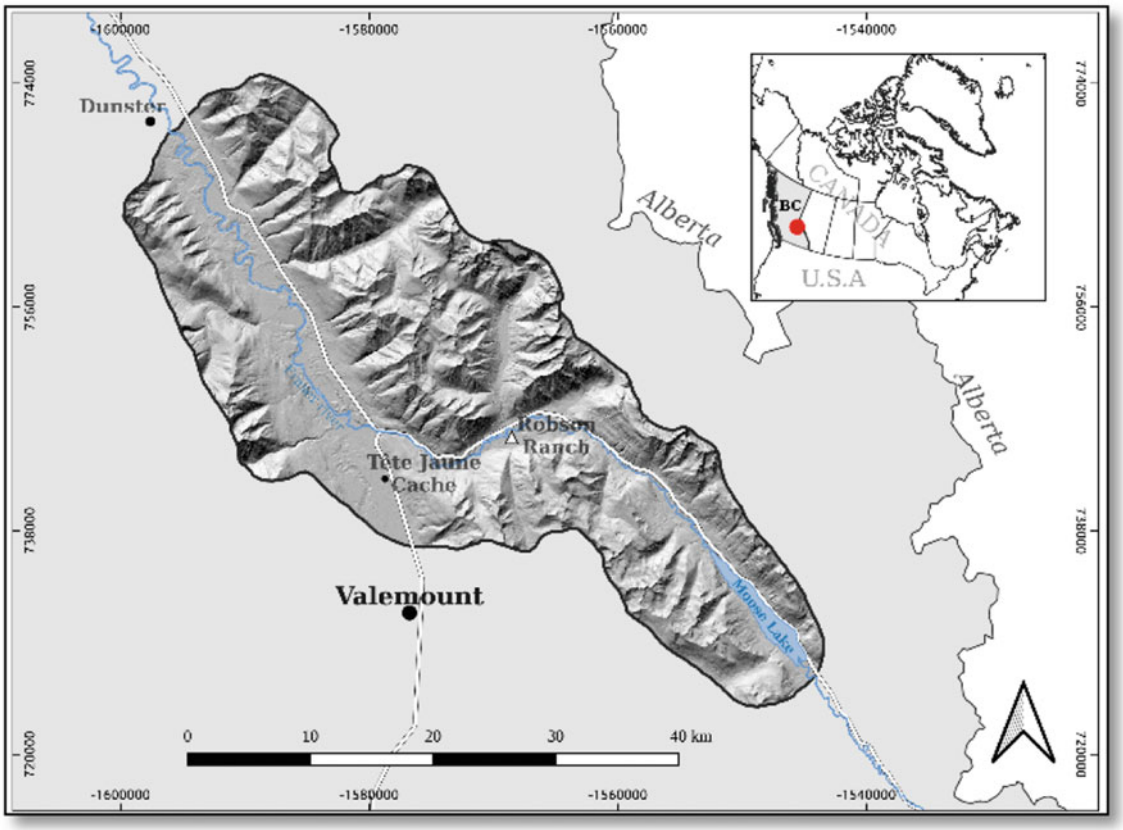

Fig. 1 Location map of the study area

The average annual precipitation at the Robson Ranch weather station is 594 mm (372.3 mm rain and 221.7 mm snow-water equivalent; Environment Canada 2022). Robson Ranch weather station is located at the bottom of the valley and may not accurately reflect the precipitation accumulation at higher elevations (Fig. 1).

Historically, the study area has witnessed several landslide events that have blocked Highway 16 and have caused damage to infrastructure. According to a report commissioned by the BC Ministry of Transportation and Highways (1999) "*several debris flows have occurred in Goslin Creek over the past 50 years*" including a May 1993 debris flow that reached Highway 16 leaving a deposit of up to 300,000 m^3. Later studies also documented the occurrence of several large deep-seated bedrock landslides in the upper basins of both Spittal and Leona creeks, with estimated return intervals of 100–500 years (MOTI 1999). Furthermore, at least six debris flow events took place between 1986 and 1997 within those two steep channels. In 2015, the BC Ministry of Transportation and Infrastructure commissioned a landslide hazard assessment for the Leona Creek landslide (BGC Engineering Inc. 2015). To provide context for their assessment, BGC Engineering Inc. (2015) conducted an inventory of nearby large ($\geq$ 1,000,000 m^3) rock landslides and documented 53 events.

These local studies indicate frequent occurrences of landslides in the study area, attesting to the need for a regional hazard assessment approach. However, there is no published regional landslide inventory available. Therefore, the objective of this study is to fill this gap by compiling a landslide inventory map that encompasses a portion of the Upper Fraser River valley.

Within, we provide a description of the data used and methodology followed to create the landslide inventory map. Our landslide inventory map (see Appendix 1, Fig. 8) is publicly available in PDF format (Bornaetxea et al. 2022) or as digital shapefiles (.shp).

2 Data

Data used for the interpretation include a digital elevation model (DEM) derived from LiDAR data, orthophotos, and geological maps. Additionally, Google Earth satellite

imagery provided support data. Analysis of the data was undertaken using QGIS software (QGIS Development Team 2022).

LiDAR Based DEMs

Since there is no publicly accessible high-resolution DEM in the study area, LiDAR data were obtained from three different sources, and combined to generate a 5 × 5 m resolution DEM (Fig. 2). This was achieved using the pdal library for laz file management and gdal library for the raster layers transformation (PDAL Contributors 2020; GDAL/OGR Contributors 2022). Details about the specific procedure followed to obtain the DEM are available in Appendix 2.

The DEM was then used to derive additional layers for use in our analysis, including contour maps with elevation intervals of 10 and 50 m, and shaded relief layers with variable azimuth light angles (commonly 45, 180, and 315°) to optimize the light orientation for terrain interpretation of different locations in the study area.

Orthophotos

Two orthophotos covered the study area (Fig. 2), 83D and 83E (1:250,000; NTS map area, 1 × 1 m resolution). These allowed for high-quality visualization of the terrain at 1:3000 scale. These color images were taken in 2005 and 2006, respectively.

Geology

As reference material, we used the Mount Robson and Canoe River geological maps published in 1980 (NTS 83E; Mountjoy 1980) and 2007 (NTS 83D; Murphy 2007) respectively, at 1:250,000 scale.

3 Methods

We prepared the landslides inventory following visual photo interpretation conventions (Guzzetti et al. 2012). Above all, the quality of the orthophotos, together with the shaded relief images allowed us to detect landslide features based on a set of characteristics such as shape, size, color, mottling, texture, pattern, site topography, and setting.

The high-resolution shaded relief images facilitate the recognition of the type of movement even in forested areas, as is evidenced from observable inactive rotational and translational landslides (Appendix 1), which would otherwise be difficult to detect using only photos (c.f. Ardizzone et al. 2007; van den Eeckhaut 2007). Debris flow and fan deposits were best observed by overlaying elevation contour lines on the hill shade images. On the other hand, the high-resolution orthophotos improved the detection of small and recent debris slides, colluvium deposits, and the delineation of debris flow initiation zones (Fell et al. 2008).

Nonetheless, we acknowledge that visual photo interpretation is considered as "*an empirical and uncertain technique that requires experience, training, a systematic methodology, and well-defined interpretation criteria*" (Guzzetti et al. 2012). For this reason, after the first landslide compilation, a verification process was completed to correct the preliminary results where needed. Furthermore, at the latter stage of the mapping process a limited field verification effort was done to confirm the accuracy of some of the mapped landslide polygons.

Landslide Type Definitions

Here, we provide a brief description of the landslide types and slope processes in the study area.

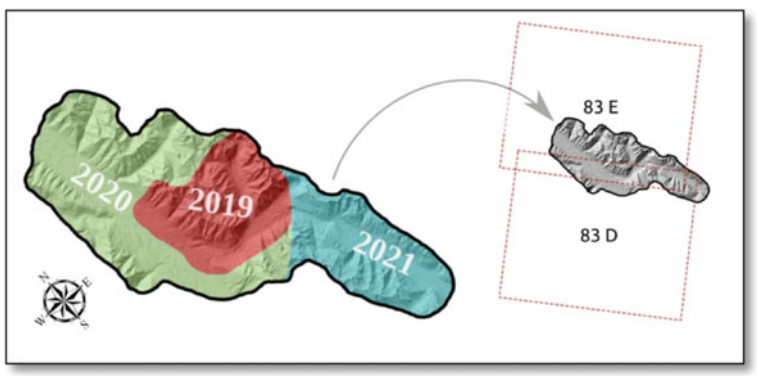

Fig. 2 Input data summary. Colored areas in the image on the left represent the different years in which LiDAR data were acquired. Dotted red lines in the image on the right represent the footprints of BC orthophotos, National Topographic System (NTS) 83D and E

Debris slide: A debris slide is a shallow movement of soil. The mobilized material usually begins moving with moderate cohesion but rapidly thereafter, cohesion diminishes and the slide mass lengthens. Usually, these landslides initiate near the crests of steep valleys. Their size typically ranges between 10^2 and 10^5 m^2.

Debris flow: A debris flow is a very rapid to extremely rapid surging flow of saturated debris in a steep channel (Hungr et al. 2014). Recognizable characteristics of debris flows include steeply sloping fans, and narrow and visibly eroded channels upstream of the fans with typically, boulder levees or train deposits on both sides of the channel. Usually, debris flows occur after periods of intense or prolonged precipitation, possibly coupled with rapid snow melt. They begin in steep sections of streams, often near the slope crests. They can be initiated by instability in the adjacent slopes, or by the instream mobilization of alluvium and debris. In a typical debris flow, the initial moving mass forms only a small portion of the final volume, with the remainder of the volume being entrained along the length of the channel (Hungr and Locat 2015).

Earthflow: Earthflows are defined as slow to rapid, flow-like movement of plastic clayey soils (Hungr et al. 2014). Thick accumulations of weathered clayey colluvium are the potential sites where earthflows can occur. Semicircular lobes at the toe of the deposits are a typical characteristic of these features.

Rock avalanche: A rock avalanche occurs when a large rock landslide on a mountain slope evolves into highly mobile mass of fragmented rock. It involves large volumes of failed material, in which the mobilized clasts collide with each other and share their momentum (Cruden and Varnes 1996).

Rockfall: A rockfall usually occurs on natural cliffs and excavation faces above transportation routes (Hungr and Locat 2015). They have rapid to extremely rapid rates of movement with the descent of material involving some freefall (Cruden and Varnes 1996). In mountainous areas, repeated detachment of rocks from steep slopes leaves exposed rock outcrops upslope and talus consisting of angular boulders and gravel at the base of the slope.

Rock slide: A slide involves displacement along a relatively thin surface of rupture (Cruden and Varnes 1996). Slides are subdivided into rotational, translational and compound types (Cruden and Varnes 1996).

Rotational slide: Rotational slides have concave upward rupture surfaces (spoon-shaped), with movement that rotates about an axis parallel to the contour of the slope (Sassa et al. 2017). The displaced mass usually moves in a relatively coherent fashion with little internal deformation. This type of slide often has an almost vertical head scarp.

Translational slides: Translational slides involve downslope movement along a relatively planar rupture surface with little or no rotation of the slide mass (Sassa et al. 2017). Translational slides commonly move along geological discontinuities such as faults, joints, bedding surfaces, or the contact between soil and rock or frozen soil. This type of slide may progress over considerable distances if the rupture surface is sufficiently inclined (Cruden and Varnes 1996).

Compound slides: Compound slides have attributes of both rotational and translational slide types (Cruden and Varnes 1996). Currently none of the mapped slides were classified as compound, but some Level 3 features may potentially be reclassified as such following field verification.

Deposit Type Definitions

To provide additional justification for our landslide mapping classifications, surficial deposits and associated landforms were also mapped. In the following paragraphs, we briefly describe their characteristics.

Coalescent debris deposit: Coalescent debris deposits are sites where multiple debris flow and debris slide deposits are superimposed upon one another, and perhaps on other sediments, forming a continuous deposit along the base of a slope.

Colluvium: Non-vegetated landslide deposits located at the base of slopes where there is no obvious source area. Colluvial deposits are generally composed of non-sorted, angular fragments of various sizes.

Talus: Rockfall deposits, comprising angular boulders, cobbles, and gravels that accumulate at the base of cliffs.

Landslide Zones

We delineated landslide paths by deposition, transportation and source, or potential source zones. Here, we provide descriptions of these zones.

Deposition: The deposition zone is where landslide sedimentation occurs. Here, the displaced material has lost kinetic energy due to a decrease in slope inclination. Deposition zones often display convex transverse profiles when compared to the adjacent, planar foot-slope area. A good example is a debris flow fan.

Transportation: The transportation zone is where colluvium transportation occurs. It connects the source and deposition zones. Additional material can be entrained from this zone during the passage of an event, leaving bare and elongated paths.

Source: The source zone is the area where displacement is initiated. Evidence for recent displacement at a source zone includes disrupted vegetation and exposed bedrock, or sediment outcrops. Depressions in the topography in steep areas are also a typical indicator of a source zone.

Potential source area: For debris flows in the study area, a source area might be the entire contributing drainage basin upstream of extensive debris flow fans. In such cases, we delineated the contributing basin as a "potential source area".

Ranking the Level of Certainty

With limited field verification, we qualitatively ranked each mapped polygon into three levels of certainty. These rankings are described below.

Level 1: This level is assigned when there is a high degree of certainty for our interpretation of the defined landslide type and delineated boundary.

Level 2: This level is assigned when either the landslide type is not certain, or its boundaries are not completely accurate due to resolution limitations of the DEM, orthophotos and satellite imagery.

Level 3: This level is assigned when there is a need for field verification. These circumstances might be the result of other possible mass-wasting processes forming the feature (e.g., rock glaciers, snow avalanche tracks, or anthropogenic slope modifications).

4 Results and Discussion

Figure 3 depicts the number of each type of mapped feature in the study area and provides the assigned ranking of the certainty level. A total of 1286 landslides and associated landforms were mapped. We found that debris flows are the most abundant feature (40%) followed by debris slides (14%) and rockfalls (11%). Furthermore, about 87% of features are assigned a certainty ranking of Level 1, 8.3% have certainty ranking of Level 2, and 4.7% have certainty ranking of Level 3.

Some specific features are entirely assigned certainty rankings of Level 2 or 3. For instance, all the coalescent debris deposits were ranked as Level 3, due to the difficulty in defining single deposits. A similar situation occurred for rock avalanches, where we classified them all as Level 2, due to difficulties in determining the nature of the mobilized material using air photo and satellite image interpretation. Differentiating between rock avalanches and rock slides was also challenging as the overall size of the displaced mass and the length of its deposits provided the only means of distinguishing the two features using our remote classification method. As a result, many rock slide—rock avalanche features area assigned certainty rankings of Level 2 or Level 3. Possible future field verification may allow us to upgrade the certainty rankings of some features.

Examples of Mapped Features

The following paragraphs provide descriptions of some of landslide types found in our study area.

Figure 4 shows an oblique perspective of an area affected by debris flows. The left image (Fig. 4a) shows several sub-basins with characteristic fan-shaped deposits at the base of a slope. Portions of the upper slope are either bare rock or sparsely vegetated suggesting recent erosion, possibly by debris flow activity. Figure 4b shows Fig. 4a, with a debris flow (certainty ranking of Level 1) source and transportation zone, and depositional zone fan at the bottom of the slope depicted by purple shading.

Figure 5 shows an oblique perspective of an area affected by debris slides. These features are found on steep slopes. The shape and size of these landslides are quite variable. Their extensive source areas suggest initial partial cohesion of the mobilized material. The debris slides stall on the slope a short distance below the initiation zone.

Debris slides are very similar to debris flows, with perhaps the principal difference being their rheology. As a result, many debris slides have been classified with certainty ranking of Level 2 due to the difficulty of clearly differentiating them from non-channelized debris flows.

Figure 6a and b show an inactive translational landslide. Thick vegetation cover obscured the landslide from view using orthophotos, suggesting that this feature has not been active for an extended period.

Although the extent of the landslide was defined with a high level of certainty (Fig. 6b), without field verification to distinguish between translational or rotational slide types, we are compelled to assign a certainty ranking of Level 2 to the classification.

Figure 7 shows coalescent debris flow deposits (green shading) and debris flows (from source area to deposition zone; purple shading). Although the coalescent fan-shaped debris flow deposits likely consist of debris flow colluvium, confirmation of this requires field-based investigations, and as such, it was assigned certainty ranking of Level 2.

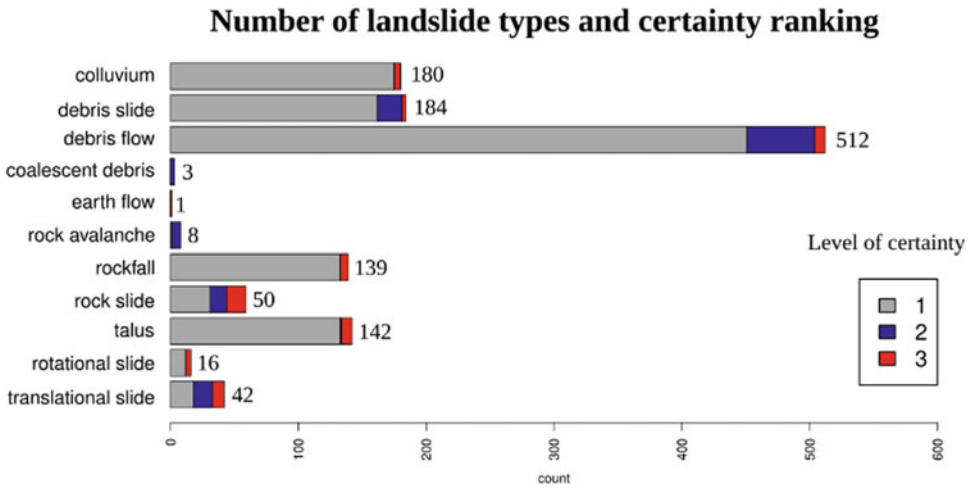

Fig. 3 Distribution of landslide types and deposits in the inventory. Horizontal bars represent the total number of features mapped for each feature type. Colors represent the proportion (%) of each feature type by level of certainty

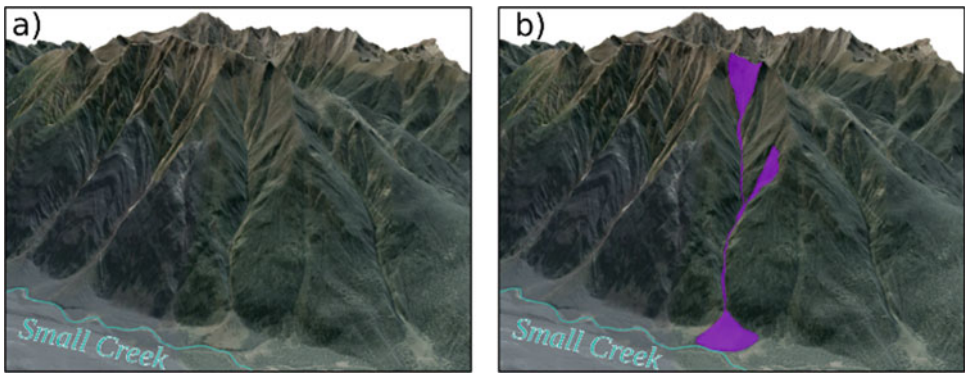

Fig. 4 **a** Oblique perspective showing a portion the study area with debris flows. **b** A debris flows source, transportation and deposition zone is shown in purple shading

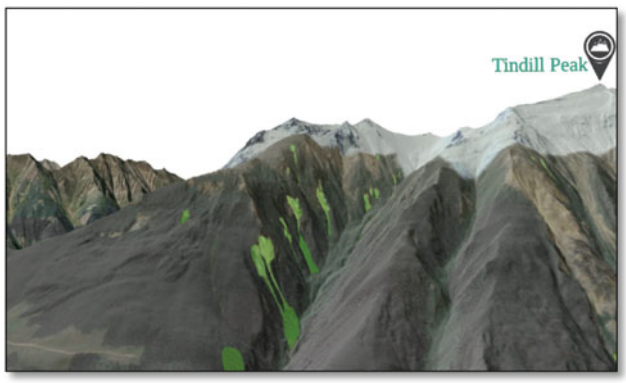

Fig. 5 Oblique perspective showing examples of debris slides (green shading)

5 Conclusions

We describe our methods for mapping landslides in the Canadian Rocky Mountains, near the town of Valemount, British Columbia, Canada.

We mapped 1286 landslides and associated landforms in a 1200 km^2 study area. The most frequent landslide types are debris flows (40%) and debris slides (14%). Eighty seven percent of features we observed were assigned the highest certainty ranking (Level 1).

This mapping project fills an information gap by providing baseline data on landslide processes and distribution for a critical infrastructure corridor in east central British Columbia. The data generated by this research will facilitate

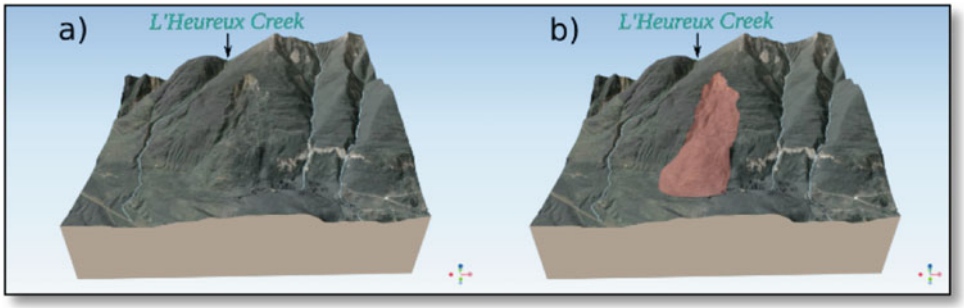

Fig. 6 **a** Oblique perspective showing a translational slide. **b** The mapped extent of the landslide is shown in salmon-colored shading

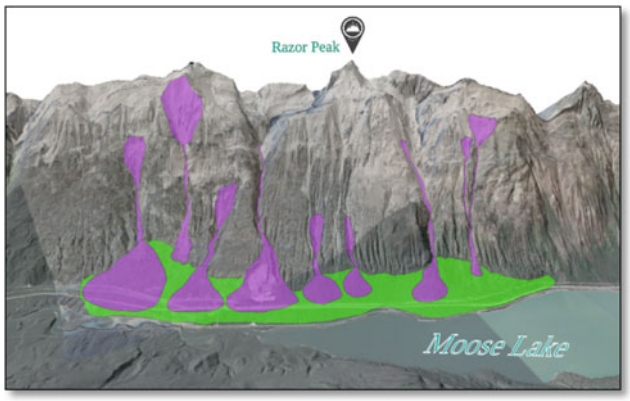

Fig. 7 Oblique perspective showing a coalescent fan-shaped debris flow deposits (green shading) and debris flows (purple shading)

future research on this and adjacent areas, and provide a reference for operational purposes.

Acknowledgements The authors want to acknowledge NRCan's Office of Energy Research and Development Project GSC-19-103 within Public Safety Geoscience Program at the Geological Survey of Canada (GSC) for providing LiDAR and field assistance. T.B. conducted much of the mapping with funding through a post-doctoral fellowship, granted by the Basque Government and the University of the Basque Country (UPV/EHU, group IT1678-22). In addition, the British Columbia Ministry of Forests provided access to LiDAR data and assistance in the field. J. Clague (Simon Fraser University) is thanked for assistance in the field. G. Hunter (British Columbia Ministry of Transportation and Infrastructure) provided assistance in the field and historic geotechnical reports. D. Huntley (GSC Pacific) peer-reviewed the paper in manuscript form. This is Geological Survey of Canada contribution number 20220201.

Appendix 1

In Fig. 8, we provide a low-resolution copy of our inventory map. The high-resolution landslide inventory map is publicly available in PDF format (Bornaetxea et al. 2022) or as digital shapefiles (.shp).

Appendix 2

Here, we provide a description of the methods used for processing our LiDAR data.

For the 2019 and 2020 data, only.laz files were available. The following data processing was undertaken to generate our final raster file in GeoTiff format:

(1) A new.laz file was created for each original file, which contained only points defined as Class 2 (ground).
(2) The files were then merged into one large file.
(3) Data were re-projected to UTM zone 11 N with WGS84 datum.
(4) A raster file of 2.5 × 2.5 m resolution was created from the LiDAR point cloud (.laz file), with the elevation value (z) being established as the lowest elevation point in the point cloud. If there were no points, then the pixel was set as NULL.
(5) For pixels that did not include an elevation value, an inverse distance weighted approach was used. For large empty areas such as lakes, a maximum number of four

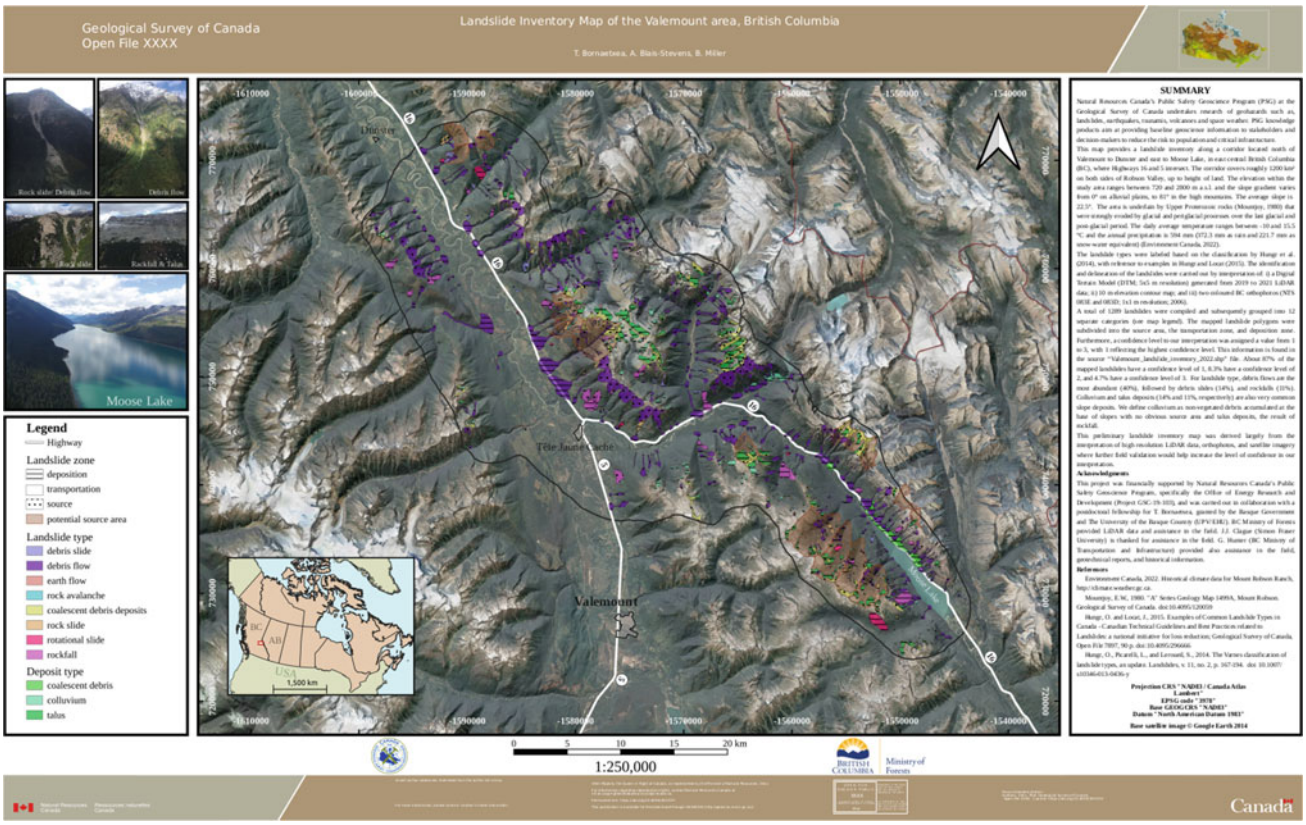

Fig. 8 Low-resolution image of our landslide inventory map for the Valemount area

consecutive pixels were used to avoid unrealistic elevation data assignments.

(6) Finally, the DEM was resampled to 5 × 5 m resolution, from 2.5 × 2.5 m resolution to satisfy the balance between resolution and file size, and to provide a smoother terrain surface for interpretation.

For the 2021 data surrounding Moose Lake, ESRI binary raster files with 1 × 1 m resolution were available. Therefore, the raster files were first transformed into generic GeoTiff format, and then resampled to 5 × 5 m resolution by means of the bilinear approach. These files were then merged with the 2019 and 2020 LiDAR files.

References

Ardizzone F, Cardinali M, Galli M, Guzzetti F, Reichenbach P (2007) Identification and mapping of recent rainfall-induced landslides using elevation data collected by airborne Lidar. Nat Hazard 7 (6):637–650. https://doi.org/10.5194/nhess-7-637-2007

BGC Engineering Inc. (2015) Leona Creek. Rock slope hazard assessment. Ministry of Transportation and Infrastructure, Vancouver, BC. p 63

Bornaetxea T, Blais-Stevens A, Miller B (2022) Landslide inventory map of the Valemount area, British Columbia. Geological Survey of Canada. Open File 8926. https://doi.org/10.4095/330911

Cruden DM, Varnes DJ (1996) Landslides: investigation and mitigation. Chapter 3-landslide types and processes. Transportation research board special report (247)

Environment Canada (2022) Historical climate data for Mount Robson Ranch weather station. http://climate.weather.gc.ca

Fell R, Corominas J, Bonnard C, Cascini L, Leroi E, Savage WZ (2008) Guidelines for landslide susceptibility, hazard and risk zoning for land-use planning. Eng Geol 102(3–4):99–111. https://doi.org/10.1016/j.enggeo.2008.03.014

GDAL/OGR Contributors (2022) GDAL/OGR geospatial data abstraction software library. Open-Source Geospatial Foundation. https://gdal.org

Guzzetti F, Mondini AC, Cardinali M, Fiorucci F, Santangelo M, Chang KT (2012) Landslide inventory maps: new tools for an old problem. Earth Sci Rev 112(1–2):42–66. https://doi.org/10.1016/j.earscirev.2012.02.001

Hungr O, Locat J (2015) Examples of common landslide types in Canada—Canadian technical guidelines and best practices related to landslides: a national initiative for loss reduction. Geological Survey of Canada, Open file 7897, p 90. https://doi.org/10.4095/296666

Hungr O, Picarelli L, Leroueil S (2014) The Varnes classification of landslide types, an update. Landslides 11(2):167–194

Massey NWD, MacIntyre DG, Desjardins PJ, Cooney RT (2005) Digital geology map of British Columbia. B.C. Ministry of Energy and Mines, Geofile 2005-1

Ministry of Transportation and Highways (1999) Hazard assessment, highway 16—Spittal and Leona Creeks, Robson District. Report submitted to the Robson District Highways Manager

Mountjoy EW (1980) "A" series geology map 1499A, Mount Robson. Geological Survey of Canada. https://doi.org/10.4095/120059

Murphy DC (2007) "A" series geology map 2110A, Canoe River, Geological Survey of Canada. https://doi.org/10.4095/223752

Natural Resources Canada (NRCAN) (2015) Seismic hazard map of Canada and local seismic hazard parameters. www.earthquakescanada.nrcan.gc.ca

PDAL Contributors (2020) PDAL point data abstraction library. https://doi.org/10.5281/zenodo.2556737

QGIS Development Team (2022) QGIS geographic information system. Open-Source geospatial foundation project. http://qgis.osgeo.org

Sassa K, Guzzetti F, Yamagishi H, Arbanas Ž, Casagli N, McSaveney M, Dang K (eds) (2017) Landslide dynamics: ISDR-ICL landslide interactive teaching tools. Volume 1: Fundamentals, mapping and monitoring. Springer

van den Eeckhaut M, Verstraeten G, Poesen J (2007) Morphology and internal structure of a dormant landslide in a hilly area: the Collinabos landslide (Belgium). Geomorphology 89(3–4):258–273. https://doi.org/10.1016/j.geomorph.2006.12.005